AD-A191 323 THOMSON SCATTERING FOR DETERMINING ELECTRON CONCENTRATIONS AND TEMPERATUR.. (U) INDIANA UNIV AT BLOOMINGTON DEPT OF CHEMISTRY K A MARSHALL ET AL. 1/1

UNCLASSIFIED 15 FEB 88 INDU/DC/GMH/RR-88-18 F/G 20/9 NL

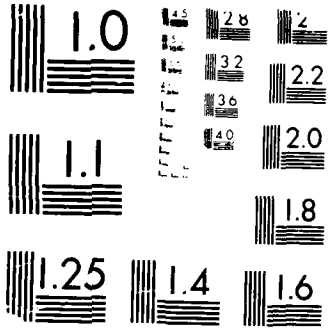


MICROCOPY RESOLUTION TEST CHART

UNCLASSIFIED



SECURITY CLASSIFICATION OF THIS PAGE

# REPORT DOCUMENTATION PAGE

AD-A191 323

1b. RESTRICTIVE MARKINGS: NA

3 DISTRIBUTION / AVAILABILITY OF REPORT: Distribution Unlimited; Approved for Public Release

2b DECLASSIFICATION / DOWNGRADING SCHEDULE: NA

4 PERFORMING ORGANIZATION REPORT NUMBER(S): INDU/DC/GMH/TR-88-18

5. MONITORING ORGANIZATION REPORT NUMBER(S): NA

6a NAME OF PERFORMING ORGANIZATION: Indiana University

6b. OFFICE SYMBOL (If applicable): NA

7a NAME OF MONITORING ORGANIZATION: ONR

6c ADDRESS (City, State, and ZIP Code): Department of Chemistry, Bloomington, IN 47405

7b ADDRESS (City, State, and ZIP Code): 800 N. Quincy Street, Arlington, VA 22217

8a NAME OF FUNDING / SPONSORING ORGANIZATION:

8b OFFICE SYMBOL (If applicable):

9 PROCUREMENT INSTRUMENT IDENTIFICATION NUMBER: Contract N00014-86-K-0366

8c ADDRESS (City, State, and ZIP Code):

10 SOURCE OF FUNDING NUMBERS

| PROGRAM ELEMENT NO. | PROJECT NO | TASK NO | WORK UNIT ACCESSION NO |
|---|---|---|---|
| | | R&T Code 4134006 | |

11 TITLE (Include Security Classification): Thomson Scattering for Determining Electron Concentrations and Temperatures in an Inductively Coupled Plasma. I. Assessment of the Technique for a Low-Flow, Low-Power Plasma

12 PERSONAL AUTHOR(S): Kim A. Marshall and Gary M. Hieftje

| 13a TYPE OF REPORT | 13b TIME COVERED | 14 DATE OF REPORT (Year, Month, Day) | 15 PAGE COUNT |
|---|---|---|---|
| Technical | FROM ____ TO ____ | 15 February 1988 | 26 |

16 SUPPLEMENTARY NOTATION: Accepted for publication in Spectrochim. Acta

| 17 COSATI CODES | | |
|---|---|---|
| FIELD | GROUP | SUB-GROUP |
| | | |
| | | |

18 SUBJECT TERMS (Continue on reverse if necessary and identify by block number): Thomson scattering; Inductively coupled plasma; Multielement analysis.

19 ABSTRACT (Continue on reverse if necessary and identify by block number)

Electron number densities and electron temperatures have been measured by multichannel Thomson scattering in a low-flow low-power inductively coupled plasma. Preliminary electron-concentration values agree well with those previously determined, and spatial variation in both electron concentration and temperature are largely consistent with existing models of the ICP. One difference is that aqueous aerosol was found here to depress the electron number density throughout the plasma. Unfortunately, the intensities measured in the wings of the Thomson-scattering spectrum exhibit large uncertainties, making data analysis difficult and the measured electron temperatures less reliable than desired.



20 DISTRIBUTION / AVAILABILITY OF ABSTRACT: ☒ UNCLASSIFIED/UNLIMITED ☐ SAME AS RPT ☐ DTIC USERS

21 ABSTRACT SECURITY CLASSIFICATION: Distribution Unlimited

22a NAME OF RESPONSIBLE INDIVIDUAL: Gary M. Hieftje

22b TELEPHONE (Include Area Code): (812) 335-2189

22c OFFICE SYMBOL:

DD FORM 1473, 84 MAR — 83 APR edition may be used until exhausted. All other editions are obsolete.

SECURITY CLASSIFICATION OF THIS PAGE

UNCLASSIFIED

OFFICE OF NAVAL RESEARCH

Contract N14-86-K-0366

R&T Code 4134006

TECHNICAL REPORT NO. 18

# THOMSON SCATTERING FOR DETERMINING ELECTRON CONCENTRATIONS AND TEMPERATURES IN AN INDUCTIVELY COUPLED PLASMA

## I. ASSESSMENT OF THE TECHNIQUE FOR A LOW-FLOW, LOW-POWER PLASMA

by

K. A. Marshall and G. M. Hieftje

Prepared for Publication

in

SPECTROCHIMICA ACTA

Indiana University
Department of Chemistry
Bloomington, Indiana 47405

15 February 1988



# 1. Introduction

The inductively coupled plasma (ICP) is an important device for analytical atomic spectrometry, and is used there as both an emission and ion source [1,2]. Unfortunately, the fundamental processes which occur in this source are not well understood. For example, it is not known whether analyte excitation and/or ionization occur by direct electron impact, by energy transfer from metastable argon, by a charge-transfer reaction, or through some other process.

A significant problem in previous attempts to achieve this understanding is the lack of available information concerning the properties and role of electrons in analytical plasmas. In the ICP, electrons are intimately involved in the energy coupling and transport processes [3,4]. The energy which sustains the ICP is coupled into the discharge by the interaction of an external radio-frequency field with electrons and ions in the plasma; the energy is more efficiently coupled to the electrons than to the ions because of their large difference in mass. The resulting energetic electrons then transfer their energy to other plasma species. In this or a subsequent energy-transfer step, the analyte species become excited and/or ionized to produce the analytical signal.

Clearly, electrons are important energy carriers in analytical plasmas. For this reason electrons have been studied extensively in the ICP [5-23]. Electron number densities have been the most thoroughly investigated electron parameter, since they are the most easily determined. In fact, it has been suggested that a comprehensive study of electron concentrations is sufficient to describe electrons in a plasma [23,24]. This assertion assumes that the energy distribution among the electrons is collisionally equilibrated and therefore Maxwellian and that

a local thermodynamic equilibrium (LTE) calculation of the electron temperature from the electron concentration is valid. This assumption might hold, but should be verified. The determination of both electron velocity distributions and number densities would indeed fully characterize electrons in the ICP. It has been suggested that the collection of this information is essential to a complete understanding of the spectral character of the plasma [25].

In the work described here, Thomson scattering is used as a diagnostic probe to measure locally both the electron concentration and electron energies in the ICP. Thomson scattering is the scattering of incident light by free electrons [26-29]. As a result, the magnitude of the scattering signal is related to the concentration of electrons in the scattering volume. Also, because these electrons move with an extremely high average velocity in the hot environment of the plasma (about $6 \times 10^5$ m/s for a 1 eV electron temperature), the scattered light is substantially Doppler shifted. This Doppler shift manifests itself in a broad spectrum of Thomson-scattered radiation whose width is related to electron energies. The Thomson-scattering spectrum thus contains information about both the electron number density and the electron energy distribution, and can be used to measure both parameters simultaneously. In addition, because the probe volume is defined by the overlap between the laser beam and the cone of light accepted by the detection optics, high spatial resolution can be obtained without the need for deconvolution procedures such as Abel inversion.

## 2. Theory

The theory of Thomson scattering is somewhat complicated and will not be covered here in detail. Conveniently, many good reviews are available on the subject [26-29]. A brief qualitative discussion is provided below so the reader can appreciate the nature of the Thomson-scattering experiment.

Thomson scattering is the scattering of radiation by electrons which are relatively free. These mobile electrons can therefore be accelerated by the electromagnetic field of incident light. As a result, the accelerated electrons themselves emit light, a process termed Thomson scattering. Of course, ions scatter light in the same manner; however, because of their greater mass, ions are accelerated by the incident electric field to a far smaller extent than electrons. The Thomson scattering they produce is therefore much weaker. Ion scattering can usually be neglected when Thomson-scattering measurements are performed.

The so-called "Thomson cross-section" is the total cross section for this scattering process in all directions ($4\pi$ sr), and is equal to $6.65 \times 10^{-25}$ cm$^2$. This small cross section indicates that the Thomson-scattering process is a rather weak phenomenon. As a result, a very intense incident light source (e.g. solid-state pulsed laser) is necessary if measurable Thomson-scattering signals are to be generated.

The power scattered, $P_s$, by a volume of electrons with a given number density, $n_e$, is given by [29]

$$P_s d\Omega d\omega = \frac{P_i r_o^2 n_e}{2\pi} L d\Omega d\omega' \left[\hat{s} \times (\hat{s} \times \hat{E}_o)\right]^2 S(\hat{k}, \omega) \qquad (1)$$

where $P_i$ is the power of the incident radiation, $r_o$ is the classical radius of an electron, L the interaction length of the incident laser beam with the scattering volume, $\hat{s}$ the unit vector in the scattering direction, $\hat{E}_o$ the electric field vector of the polarized incident laser beam, $d\Omega$ and $d\omega$ are the differential solid angle and differential frequency interval, respectively, and $s(\hat{k}, \omega)$ is the spectral density function which describes the frequency dependence of the scattering spectrum.

If the electrons in the scattering volume are stationary, no Doppler shift occurs and the spectral density function is 1 at $\omega=0$ (no frequency shift) and zero at all other frequencies. Of course, this situation is very unlikely since even at room temperature the kinetic energy of free electrons would provide them with an average velocity of almost $10^5$ meters per second. A substantial Doppler shift is therefore observed in the spectrum of the radiation scattered by electrons moving in a hot plasma. The spectral density function, which describes this Doppler-shifted spectrum, is very complicated and a description of it is beyond the scope of this treatment. Details on this function can be found elsewhere [28].

If the probed electrons are completely free and exhibit a collisionally equilibrated Maxwellian velocity distribution, the Thomson scattering spectrum will be Gaussian in shape and centered at the wavelength of the incident radiation. However, if the electrons are not completely free--that is, if their motion is correlated with the motion of other electrons or with the motion of ions, the shape of the scattering spectrum will deviate from Gaussian. The degree to which this

deviation occurs is determined by the scattering parameter $\alpha$, which is given by

$$\alpha = \frac{\lambda_o}{4\pi\ \lambda_D\ \sin(\frac{\theta}{2})} \tag{2}$$

where $\lambda_o$ is the incident laser wavelength, $\theta$ is the scattering angle, and $\lambda_D$ is the so-called Debye shielding length. The Debye length is

$$\lambda_D = \left(\frac{k\ T_e}{4\pi\ e^2 n_e}\right)^{1/2} \tag{3}$$

where k is the Boltzmann constant, $T_e$ the electron temperature, $n_e$ the electron concentration, and e the charge on an electron. This shielding length is the characteristic distance in the plasma over which an electrostatic potential is shielded by neighboring charges.

Because the spectral density function depends on $\alpha$, so does the shape of the scattering spectrum. Fortunately, there is some experimental control over $\alpha$. The value of $\alpha$ depends not only on the electron concentration and temperature (which are the targets of the measurement and therefore cannot be controlled), but also on the scattering angle $\theta$. For a given set of plasma conditions, a larger scattering angle produces a smaller $\alpha$. If the "true" electron energy distribution and the average velocity are both to be determined, it is important to keep $\alpha$ as small as possible. A large scattering angle is therefore desirable.

## 3. Experimental

A detailed description of the experimental apparatus used in this work is given in a companion paper [30]. Accordingly, only a brief overview is presented below.

A Q-switched ruby laser with an output power of approximately 20 MW (0.5 joules/pulse) provides the incident 25-ns light pulse at 694.3 nm. The laser beam is focused to a 1.3-mm spot in the plasma. A rotating-mirror optical chopper is used to protect the photomultiplier tubes (PMTs) from the intense continuum and line background emission produced by the ICP. The laser pulse is synchronized with the 25-$\mu$s optical gate produced by this chopper. A 1-m Czerny-Turner spectrometer equipped with a 2400 groove/mm holographically ruled grating is used to collect the scattering signal.

A 25-channel fiber-optic array is mounted in the focal plane of the spectrometer. The center channel of this array is positioned at the ruby-laser wavelength (694.3 nm) and monitors Rayleigh scattering; the remaining channels are used for Doppler-shifted Thomson-scattering measurements. The pigtail outputs of the fiber-optic array are connected to individual photomultiplier tubes, each of which is sampled by its own gated-integrator module. The voltage outputs from the gated-integrator cards are digitized and sent to a host laboratory computer for storage and data analysis.

The response factors of the different detection channels are normalized by collecting many pulses from a red light-emitting diode (LED), which is mounted inside the spectrometer. The measured normalization factors are then used to correct the observed Thomson-scattering intensities for instrumental response.

The plasma is supported by a 2.5 kW, 27.12 MHz radio-frequency generator. All gas flows were metered by a mass-flow controller. The

plasma conditions used in this study were 875 W incident power, 12.0 l/min outer gas flow, 0.50 l/min intermediate gas flow, and 0.60 l/min inner gas flow. When water was nebulized into the plasma, a flow rate of 2 mL/min was directed to a glass-concentric nebulizer by a peristaltic pump. The ICP torch was of a demountable low-flow low-power design similar in geometry and internal size to that described by REZAAIYAAN and HIEFTJE [31].

## 4. Results and Discussion

Data Treatment

If a Thomson-scattering spectrum has a Gaussian shape (Fig. 1), the area under the Gaussian curve can be used to calculate the electron concentration in the scattering volume, while the width of the spectrum indicates the average electron energy (or electron temperature). The electron concentration can be calculated from

$$n_e = C_{Inst} \int I_T d\lambda \cdot (1 + \alpha^2) \qquad (4)$$

where $n_e$ is the electron number density, $C_{inst}$ an instrument-response constant, $I_T$ the wavelength-dependent Thomson-scattering intensity, and $\alpha$ the scattering parameter described earlier.

In the multi-channel instrument [30], a scattering spectrum is divided into 25 discrete channels, with adjacent channels being separated by a small spacer (Fig. 1). Consequently, a continuous, complete Thomson-scattering spectrum is not available. Furthermore, the

central (laser wavelength) channel cannot be used because of the intense Rayleigh-scattered radiation that strikes it. Therefore, the intensity of the Thomson-scattering component in this central channel must be inferred from the signal obtained in the adjacent Doppler-shifted channel. Afterward, the intensity summation under the Thomson-scattering spectrum can be approximated as

$$\int I_T \, d\lambda = 1/2 \; Ch(1) + 5/4 \sum_{i=1}^{11} Ch(i) \qquad (5)$$

where Ch(i) is the measured scattering intensity in integrator channel "i". In Eqn 5, the factor 5/4 accounts for the fact that individual measurement channels are separated by a spacer that is one-quarter their width [30]. The factor of 1/2 in the first term results from the central channel, positioned at the Rayleigh wavelength, receiving a contribution from both halves of the Thomson spectrum.

The instrumental response constant ($C_{inst}$) in Eqn 4 must be known before the summation in Eqn 5 can be used to calculate the electron concentration. A simple way of determining this response constant is to use the Rayleigh-scattering signal obtained from room-temperature atmospheric-pressure argon as a calibration signal [20,30]. From this calibration procedure, Eqn 4 becomes

$$n_e = \frac{\int I_T d\lambda}{I_{Rv}} \quad \frac{\sigma_{Ar}}{\sigma_T} \quad n_{Ar} \; (1 + \alpha^2) \qquad (6)$$

where $I_{Ry}$ is the Rayleigh-scattering intensity from room-temperature atmospheric-pressure argon with number density $n_{Ar}$, $\sigma_{Ar}$ the total Rayleigh-scattering cross section for argon, and $\sigma_T$ the total Thomson-scattering cross section.

Calculation of an electron temperature from a Gaussian Thomson spectrum is straightforward. If the electron energy distribution is Maxwellian and the scattering parameter $\alpha$ is small ($\alpha < 0.2$), the electron temperature ($T_e$) can be determined from the slope of a plot of the natural logarithm of the scattering intensity against the square of the wavelength shift [28]. The slope of this plot is given by

$$\text{Slope} = \frac{-6.39 \times 10^{4}}{\lambda_o^2} \left[\sin^2 \left( \frac{\theta}{2} \right) T_e\right]^{-1} \qquad (7)$$

where $\lambda_o$ is the wavelength of the incident radiation, expressed in the same units (nm) as the wavelength shifts used in the linear plot, and $\theta$ is the scattering angle.

Unfortunately, noise in the weak wings of a scattering spectrum greatly affects temperatures determined by this slope approach; the slope of the line is influenced equally by all the data points. In contrast, the calculation of electron concentrations is not similarly affected; the area under the scattering spectrum is relatively immune to variations in the weaker portions of the scattering signal. As a consequence, electron number density can be determined with greater confidence than electron temperature. Understandably, the most reliable electron temperatures are calculated from only the points in the more intense center of the scattering spectrum.

These features are illustrated by the linearized Thomson-scattering spectrum of Fig. 2. If the left-most eight points in Fig. 2 are used to calculate an electron temperature, a lower value (7400 K) is obtained than if all of the points in the plot are used (9700 K). Obviously, the calculated electron temperature depends strongly on which portion of the spectrum is used in the calculation. In fact, the decision to include a particular point in the calculations can affect the measured temperature by as much as 300 K. In the linearized spectrum plotted in Fig. 2, there is no apparent break in the line. In some cases, however, a clear break can be seen and the decision of which data points to use in the calculation of the slope is more obvious. In addition, the curvature found in many spectra is not as great as that found in Fig. 2 and the points to be selected are not as critical.

Two fundamental reasons could account for the nonlinearity of Fig. 2--a non-Maxwellian electron velocity distribution or a large value of the scattering parameter $\alpha$. The value for $\alpha$ calculated from the data depicted in Fig. 2 is 0.28 and should distort the shape of the scattering spectrum by less than 8% (the intensity scales as $1 + \alpha^2$). Moreover, the direction of curvature in Fig. 2 is opposite to what would be expected if large $\alpha$ values produced the nonlinearity. As $\alpha$ increases, the center of the scattering spectrum becomes dampened (reduced in intensity), while the tail of the scattering spectrum is relatively unaffected for $\alpha$ less than about 0.5 [29]. In Fig. 2, the central two points are actually reduced in magnitude by errors attributable to the residual contribution of Rayleigh scattering. The remaining points in Fig. 2 exhibit curvature in a direction opposite to that which a large value of $\alpha$ would produce.

Although departure from a Maxwellian electron energy distribution could produce the kind of nonlinearity seen in Fig. 2, the deviations observed here are much greater than could logically be anticipated. The most probable deviation from a Maxwellian electron velocity distribution is an enhancement or depletion of the high-energy tail of the distribution [32]. Consequently, the far wings of the Thomson-scattering spectrum would be similarly enhanced or depleted. In an atmospheric-pressure plasma such as the ICP, electron energy exchange processes should be collisionally dominated, and deviations from a Maxwellian velocity distribution (if any) should be small. In addition, the effect of a particular deviation on the spectral shape would not be as large as the actual change in the velocity distribution. This is because scattering signals produced by the high-velocity electrons do not occur exclusively in the wings of the scattering spectrum; the Thomson-scattering spectrum results from a combination of both electron speed and direction of travel. That is, only the component of a given electron's velocity which is in the direction of the so-called differential scattering vector (determined by scattering geometry) produces a signal at a particular Doppler-shifted wavelength.

One kind of deviation from a Maxwellian energy distribution which would exhibit the nonlinearity apparent in Fig. 2 is the simultaneous existence of two electron populations, each with a Maxwellian energy distribution but with a different average velocity (electron temperature). This situation has been observed in low-pressure high-temperature plasmas [33], but would not be expected to occur in the ICP. The high pressure and electron-collision rate in the ICP should produce energy exchange at a rate

that is too high to allow the existence of two highly populated independent energy distributions.

The most likely cause for the nonlinear curve in Fig. 2 is instrumental in nature. First, the observations could be explained by an uncorrected offset in the baseline or zero signal level, caused in turn by incomplete subtraction of stray light and ICP background radiation. Second, the points in the tail of the scattering spectrum are probably biased high in part because there is a limit to a signal variation that can be measured in the negative direction but no similar limit for positive deviations.

In the results presented below, the portion of the Thomson-scattering spectrum which was used to calculate an electron temperature was selected somewhat subjectively. Although this procedure is less than desirable, it provides useful results for this preliminary investigation.

Measured Values

Measured electron concentrations, electron temperatures, the $r^2$ values from the line used to calculate $T_e$, and the number of points (N) used to calculate the least-squares line are presented in Table 1. Also listed in this table are the calculated "LTE" electron temperatures obtained by inserting the determined electron number densities into the Saha equation [34,35]:

$$\frac{n_i n_e}{n_a} = \frac{(2\pi m k T_e)^{3/2}}{h^3} \frac{2Z_i}{Z_a} \exp\left(\frac{-E_i}{kT_e}\right) \qquad (8)$$

In Eqn 8, $n_i$, $n_e$, and $n_a$ are, respectively, the localized number densities of the ions, electrons, and atoms. $Z_i$ and $Z_a$ are the partition functions of the ion and atom, $E_i$ is the ionization energy, m is the electron mass, k is the Boltzmann constant and h is Planck's constant. In Eqn 8, $T_e$ should actually be an ionization temperature, but in assuming LTE in these calculations we can take this value to be the electron temperature. The argon atom number density $n_a$ can be calculated from the ideal-gas law and can be assumed to be relatively unchanged by the small fraction of ions (0.1%) which exist in the typical ICP. The argon ion number density can be assumed to be the same as the electron concentration since argon is the predominant source of electrons. The partition functions have been tabulated by de Galan et al [36].

Table 1 also includes gas temperatures which were determined in our laboratory by Rayleigh-scattering measurements [37]. These values represent "true" gas-kinetic temperatures and as such are the lower limit expected for the electron temperature. Note that in all but one case, where S/N was low, the measured electron temperature is higher than the gas temperature.

The large uncertainties in the measured electron temperatures (as much as 25%) are due to noise in the scattering spectra and to the subjective method used in the slope method of determination (see Fig. 2). Indeed, if this subjective selection process is abused, it is possible to tune the determined electron temperature almost at will. In the results presented here we attempted to avoid this ambiguity by selecting data from the inner 6 to 9 points in the Doppler-shifted scattering spectrum. The $r^2$ values obtained in the least-squares fit of

the selected points were used to help gauge which points should be selected. The linear fit was made as good as possible at the same time the number of data points (N) used from the scattering spectrum was maximized.

Because of the large uncertainty in the electron temperature values reported here, no analysis of the spatially resolved electron-energy features was attempted. However, it is important to note that the electron temperatures determined here follow trends similar to those found in gas temperatures measured in the same low-flow low-power torch (Table 1 and ref. 37), and that the electron temperatures are usually 2000-3000 K higher than the gas temperatures determined under the same conditions. These trends are not surprising.

Figure 3 shows electron concentrations in an 875 W low-flow low-power plasma as a function of vertical position. The uncertainties in the measured electron concentration are less than 10%. Thus, the apparent differences between the on-axis electron number densities that are measured in the presence and absence of water vapor are significant. Interestingly, electron concentrations measured on the plasma axis and near the load coil are slightly lower when aerosol is introduced. This trend is opposite from that found by KIRKBRIGHT [38]. In contrast, values obtained off axis or higher in the plasma are less affected by the introduction of water aerosol. These trends might be the result of a decrease in the plasma-gas temperature produced by the introduction of water in the plasma (see Table 1 and ref. 37).

An expected trend in Fig. 3 is the reduction in electron concentration with height in the plasma. The highest electron concentrations should exist in the plasma fireball; the concentration should decrease as the plasma

decays (at higher positions). Overall, the magnitude of our electron number densities agrees with those found by CAUGHLIN and BLADES [17,23] although their electron concentrations were determined in a conventional ICP torch and at a higher power (1 kW).

Although the data presented here are preliminary and the dependability of the measured electron temperatures is not yet acceptable, we feel that Thomson scattering shows great promise. With further improvements in the instrumental system and data-manipulation procedures, the determined electron concentrations and temperatures should become quite reliable. In particular, a new Nd:YAG pulsed laser is being incorporated into the scattering system. The high repetition rate of this laser will allow signal averaging over hundreds or thousands of laser pulses compared to the tens of pulses averaged with the present system.

## ACKNOWLEDGEMENT

The authors are grateful to GEORGE E. EWING for use of the ruby laser employed in this study. Supported in part by the National Science Foundation through grant CHE 83-20053, by the Office of Naval Research, and by American Cyanamid.

## REFERENCES


[1] P.W.J.M. Boumans, ed., Inductively Coupled Plasma Emission Spectroscopy, Part I: Methodology, Instrumentation, and Performance, Part II: Applications and Fundamentals, Wiley, New York (1987).

[2] D. J. Douglas and R. S. Houk, Prog. Analyt. Atom. Spectrosc. 8, 1 (1985).

[3] V. A. Fassel and R. N. Kniseley, Anal. Chem. 46, 1155A (1974).

[4] S. Greenfield, H. McD. McGeachin and P. B. Smith, Talanta 22, 553 (1975).

[5] J. M. Mermet, Spectrochim. Acta 30B, 383 (1975).

[6] J. Jarosz and J. M. Mermet, J. Quant. Spectrosc. Radiat. Transfer 17, 237 (1977).

[7] D. J. Kalnicky, V. A. Fassel and R. N. Kniseley, Appl. Spectrosc. 31, 137 (1977).

[8] J. Jarosz, J. M. Mermet and J. P. Robin, Spectrochim. Acta 33B, 55 (1978).

[9] A. Montaser, V. A. Fassel and G. Larsen, Appl. Spectrosc. 35, 385 (1981).

[10] A. Batel, J. Jarosz and J. M. Mermet, Spectrochim. Acta 36B, 983 (1981).

[11] F. Aeschbach, Spectrochim. Acta 37B, 987 (1982).

[12] A. Batal, J. Jarosz and J. M. Mermet, Spectrochim. Acta 37B, 511 (1982).

[13] Y. Nojiri, K. Tanabe, H. Uchida, H. Haraguchi, K. Fuwa and J. D. Winefordner, Spectrochim. Acta 38B, 61 (1983).

[14] W. H. Gunter K. Visser and P. B. Zeeman, Spectrochim. Acta 38B, 949 (1983).

[15] B. L. Caughlin and M. W. Blades, Spectrochim. Acta **39B**, 1583 (1984).

[16] S. R. Goode and J. P. Deavor, Spectrochim. Acta **39B**, 813 (1984).

[17] B. L. Caughlin and M. W. Blades, Spectrochim. Acta **40B**, 987 (1985).

[18] M. W. Blades and B. L. Caughlin, Spectrochim. Acta **40B**, 579 (1985).

[19] L. J. Prell, C. Monnig, R. E. Harris, and S. R. Koirtyohann, Spectrochim. Acta **40B**, 969 (1985).

[20] H. Huang, K. A. Marshall and G. M. Hieftje, Anal. Chem. **58**, 207 (1986).

[21] E. H. Choot and G. Horlick, Spectrochim. Acta **41B**, 889 (1986).

[22] E. H. Choot and G. Horlick, Spectrochim. Acta **41B**, 907 (1986).

[23] I. J. M. M. Raaijmakers, P. W. J. M. Boumans, B. van der Sijde and D. C. Schram, Spectrochim. Acta **38B**, 697 (1983).

[24] M. W. Blades, B. L. Caughlin, Z. H. Walker and L. L. Burton, Prog. Analyt. Spectrosc. **10**, 57 (1987).

[25] G. D. Rayson and G. M. Hieftje, Spectrochim. Acta, **41B**, 683 (1986).

[26] D. E. Evans and J. Katzenstein, Rep. Prog. Phys. **32**, 207 (1969).

[27] A. W. DeSilva and G. C. Goldenbaum, Methods of Experimental Physics, **Vol. 9A**, Ed. H. R. Griem and R. H. Louberg. Academic Press, New York, (1970).

[28] J. Sheffield, Plasma Scattering of Electromagnetic Radiation, Academic Press, New York (1975).

[29] A. Scheeline and M. J. Zoellner, Appl. Spectrosc. **38**, 245 (1984).

[30] K. A. Marshall and G. M. Hieftje, Spectrochim. Acta **43B**, 000 (1988).

[31] R. Rezaaiyaan and G. M. Hieftje, Anal. Chim. Acta **173**, 63 (1985).

[32] J. J. A. M. van der Mullen, Excitation Equilibria in Plasmas, Ph.D. Thesis, University of Technology, Eindhoven (1986).

[33] L. Pieroni and S. E. Segre, Phys. Rev. Lett. **34**, 928 (1975).

[34] P.W.J.M. Boumans, Theory of Spectrochemical Excitation, Hilger/London, Plenum/New York (1966).

[35] M. W. Blades, Excitation Mechanisms and Discharge Characteristics--Recent Developments, Inductively Coupled Plasma Emission Spectroscopy (Ed. P.W.J.M. Boumans), Part II: Applications and Fundamentals, Chapter 11, p. 387. Wiley, New York (1987).

[36] L. de Galan, R. Smith, and J. D. Winefordner, Spectrochim. Acta 23B, 521 (1968).

[37] K. A. Marshall and G. M. Hieftje, J. Anal. Atom. Spectrom. (in press, 1987).

[38] G. F. irkbright, Developments in Atomic Plasma Spectrochemical Analysis, p. 223, Ed. R. M. Barnes, Heyden, London (1981).

**TABLE 1**

Temperatures and Electron Concentrations in an 875-watt Low-Flow Low-Power ICP

| Height ALC (mm) | $T_{gas}$[a] (K) | $T_e$ (K) | N[b] | $r^2$[c] | $n_e$ ($\times 10^{14}$ $cm^{-3}$) | LTE $T_e$[d] (K) |
|---|---|---|---|---|---|---|
| On plasma axis no aerosol: | | | | | | |
| 5 | 7300 | 11400 | 9 | 0.983 | 23 | 8300 |
| 10 | 7500 | 9000 | 9 | 0.982 | 18 | 8100 |
| 15 | 7200 | 7500 | 7 | 0.958 | 6.8 | 7500 |
| 20 | 5700 | -- | -- | -- | 0.65 | 6300 |
| On plasma axis with aerosol: | | | | | | |
| 5 | 7000 | 9600 | 8 | 0.984 | 17 | 8100 |
| 10 | 7300 | 9600 | 8 | 0.979 | 16 | 8000 |
| 15 | 6900 | 9400 | 9 | 0.960 | 5.6 | 7400 |
| 20 | 6300 | -- | -- | -- | 0.63 | 6300 |
| 3 mm off plasma axis no aerosol: | | | | | | |
| 5 | 7200 | 10700 | 9 | 0.989 | 19 | 8100 |
| 10 | 7200 | 9400 | 9 | 0.973 | 13 | 7900 |
| 15 | 6700 | 8200 | 7 | 0.982 | 7.6 | 7500 |
| 20 | 6400 | 6300 | 6 | 0.984 | 1.3 | 6600 |
| 3 mm off plasma axis with aerosol: | | | | | | |
| 5 | 7800 | 9600 | 9 | 0.979 | 18 | 8100 |
| 10 | 7200 | 9100 | 6 | 0.951 | 14 | 7900 |
| 15 | 6700 | 8900 | 7 | 0.984 | 7.4 | 7500 |
| 20 | 6400 | 9100 | 6 | 0.960 | 1.5 | 6600 |

[a]Gas temperature from reference [37].

[b]The number of data points used in the least-squares fit of the data. A complete Thomson spectrum contains 12 points here.

[c]Correlation for the least-squares fit of the slope determination.

[d]"LTE" electron temperature determined from the Saha equation.

## FIGURE LEGENDS

Fig. 1. How a hypothetical Thomson-scattering spectrum falls on the channels of the fiber-optic array.

Fig. 2. Linearized form of a Thomson-scattering spectrum taken at 10 mm above the ICP load coil and 3 mm off axis. The slope of the line is used to calculate the electron temperature, but different slopes can be calculated from this line because of its curvature.

Fig. 3. Measured electron number density as a function of height in an 875 W low-flow low-power plasma. The circles are for data taken on the plasma axis, and the triangles for data taken 3-mm off the plasma axis. The closed symbols are electron concentrations in a plasma with no water aerosol introduced into it, and the open symbols for a plasma in which an aqueous aerosol has been introduced into the central channel.

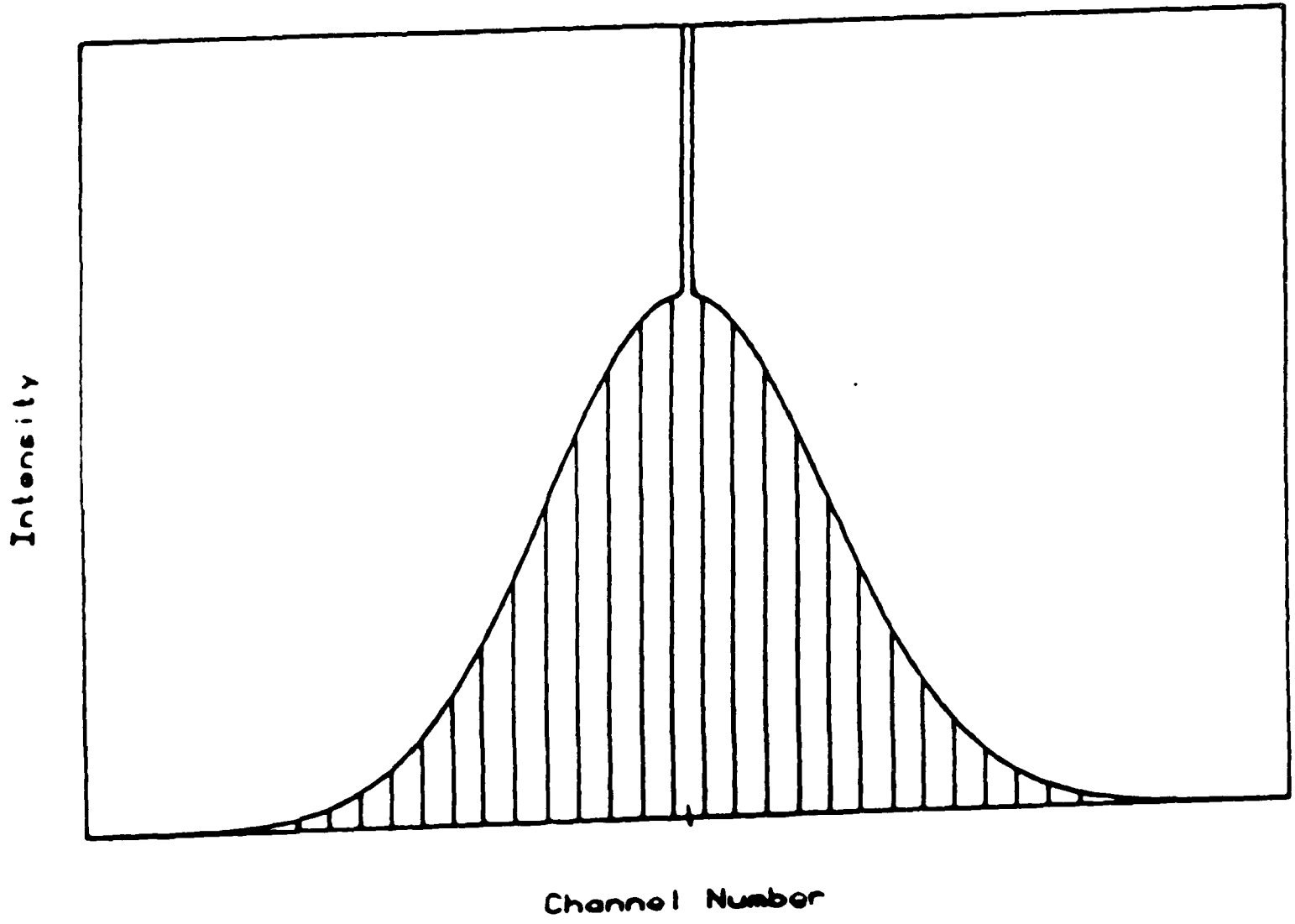


Fig. 1

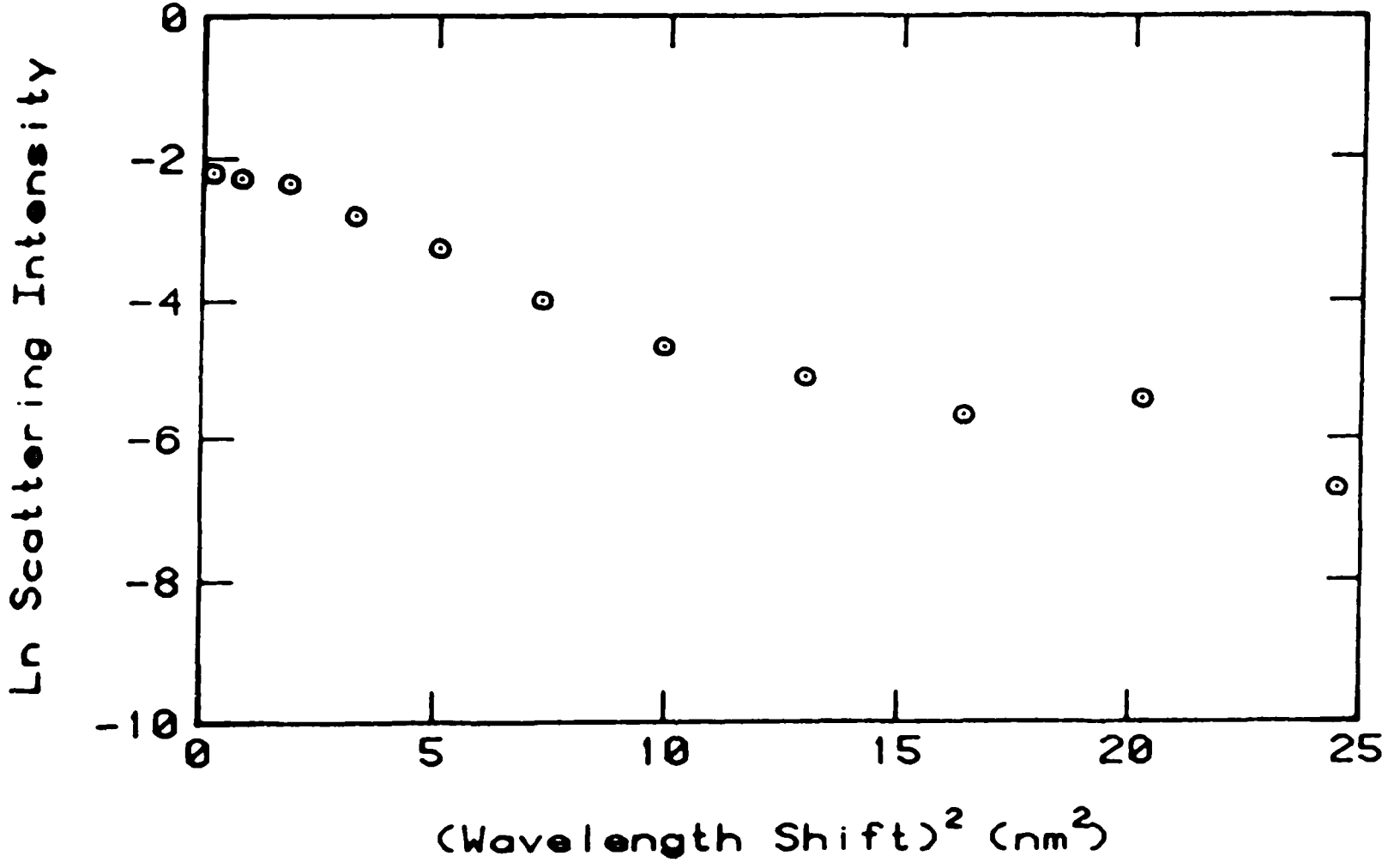
Ln Scattering Intensity
0
-2
-4
-6
-8
-10
0
5
10
15
20
25
(Wavelength Shift)$^2$ (nm$^2$)

Fig. 2

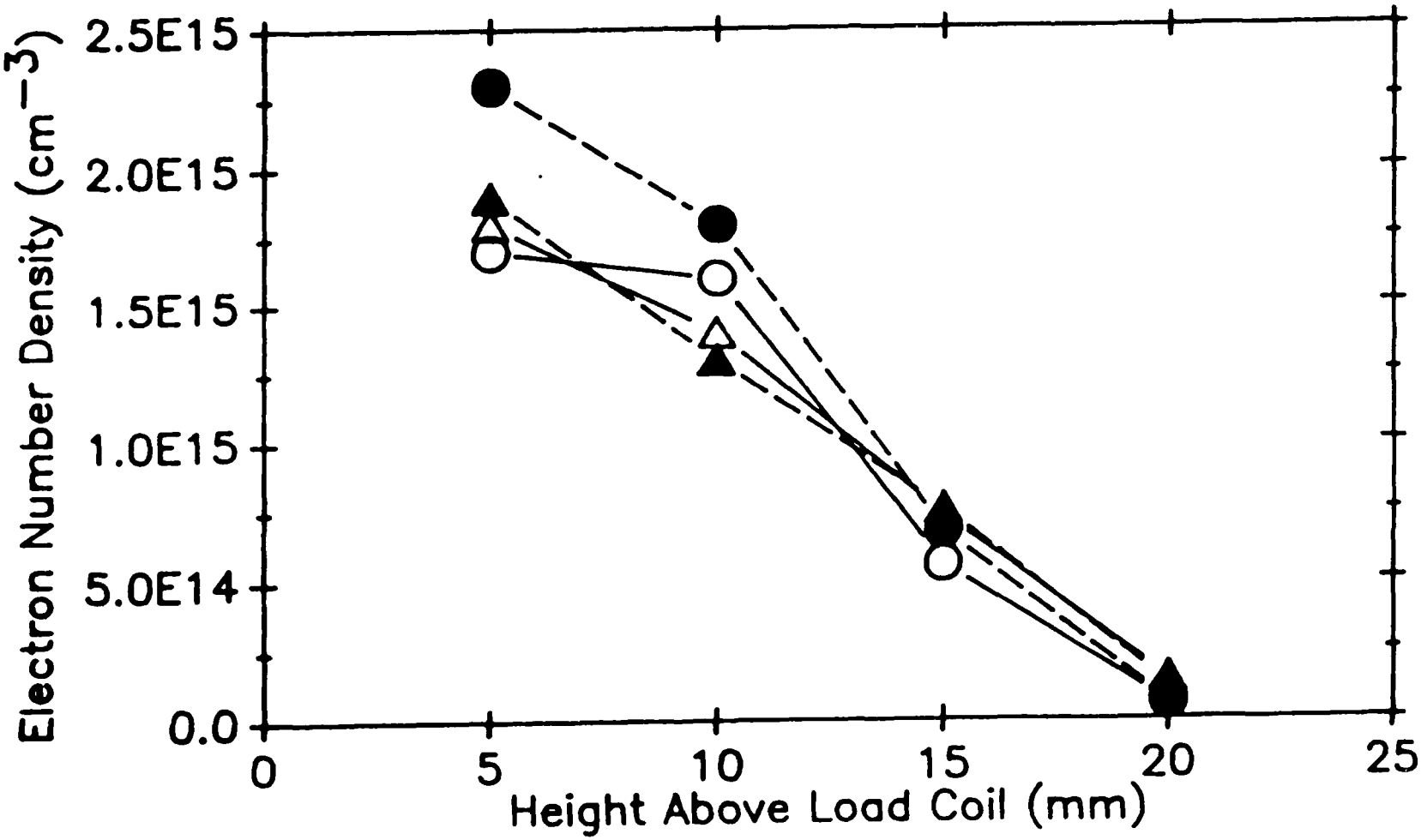
Electron Number Density ($cm^{-3}$)
2.5E15
2.0E15
1.5E15
1.0E15
5.0E14
0.0
0
5
10
15
20
25
Height Above Load Coil (mm)

Fig. 3

# TECHNICAL REPORT DISTRIBUTION LIST, GEN

| | No. Copies |
|---|---|
| Office of Naval Research<br>Attn: Code 1113<br>800 N. Quincy Street<br>Arlington, Virginia 22217-5000 | 2 |
| Dr. Bernard Douda<br>Naval Weapons Support Center<br>Code 50C<br>Crane, Indiana 47522-5050 | 1 |
| Naval Civil Engineering Laboratory<br>Attn: Dr. R. W. Drisko, Code L52<br>Port Hueneme, California 93401 | 1 |
| Defense Technical Information Center<br>Building 5, Cameron Station<br>Alexandria, Virginia 22314 | 12 high quality |
| DTNSRDC<br>Attn: Dr. H. Singerman<br>Applied Chemistry Division<br>Annapolis, Maryland 21401 | 1 |
| Dr. William Tolles<br>Superintendent<br>Chemistry Division, Code 6100<br>Naval Research Laboratory<br>Washington, D.C. 20375-5000 | 1 |
| Dr. David Young<br>Code 334<br>NORDA<br>NSTL, Mississippi 39529 | 1 |
| Naval Weapons Center<br>Attn: Dr. Ron Atkins<br>Chemistry Division<br>China Lake, California 93555 | 1 |
| Scientific Advisor<br>Commandant of the Marine Corps<br>Code RD-1<br>Washington, D.C. 20380 | 1 |
| U.S. Army Research Office<br>Attn: CRD-AA-IP<br>P.O. Box 12211<br>Research Triangle Park, NC 27709 | 1 |
| Mr. John Boyle<br>Materials Branch<br>Naval Ship Engineering Center<br>Philadelphia, Pennsylvania 19112 | 1 |
| Naval Ocean Systems Center<br>Attn: Dr. S. Yamamoto<br>Marine Sciences Division<br>San Diego, California 91232 | 1 |

END

DATE

FILMED

5-88

DTIC